Journal of Nonlinear Modeling and Analysis
Volume 7, Number 6, December 2025, 2001–2012
https://journal.global-sci.org/jnma
DOI:10.12150/jnma.2025.2001

The Second-Order Melnikov Function and Chaotic Tangles on Toral van der Pol Equation*

Fengjuan Chen[1,†], Mei Chen[1] and Yi Zhong[2]

Abstract The van der Pol equation on the torus is considered. This equation contains a heteroclinic cycle consisting of four symmetric heteroclinic orbits. By high order Melnikov method, the periodic forced van der Pol equation is investigated and chaotic dynamics is obtained. An explicit formula of the second-order Melnikov function is derived for the splitting heteroclinic connection. It is used to detect chaotic dynamics when the first-order(classical) Melnikov function is degenerate. By the second-order Melnikov function, we deduce chaotic heteroclinic tangles with rigorously theoretical analysis as well as numerical simulations.

Keywords Van der Pol equation, high order Melnikov method, heteroclinic tangles

MSC(2010) 37C29, 34E10, 34C28, 34C37.

1. Introduction

As we have known, the planar van der Pol equation provides a typical example of relaxation oscillators which possess limit cycles by Poincaré-Bendixson theorem [1]. For the strongly forced van der Pol equation, Levinson [2] and Levi [3] noted that there exists an attracting set involving homoclinic tangles. In the 1960s, Smale observed that horseshoe, which represents chaos in the sense of topology, occurs in all homoclinic tangles [4]. Recently, Refs. [5–7] presented that periodic sinks and Hénon-like attractors are also residing in homoclinic and heteroclinic tangles.

Melnikov's method is one of the few analytical methods available for the detection of chaotic motions [1,8–11]. This method establishes a basic Melnikov function $M_0(t_0)$ to check the existence of transverse homoclinic points by simple zeros. However, there exist equations such that $M_0(t_0)$ is degenerate. In this case we need to consider high order Melnikov functions to analyze the separation between stable and unstable manifolds. Although Ref. [12, 13] proposed a scheme to derive high order Melnikov functions, it is hard for one to apply in the concrete examples. Recently, Refs. [14–17] developed an entire theory of high order Melnikov functions

†the corresponding author.
Email address:fjchen@zjnu.cn(F. Chen),
meichen@zjnu.edu.cn(M. Chen), yizhong@zju.edu.cn(Y. Zhong)
[1]Department of Mathematics, Zhejiang Normal University, Jinhua, Zhejiang 321004, China
[2]Institute of Mathematical Sciences and Applications, NingboTech University, Ningbo 315100, China
*The work was supported by the National Natural Science Foundation of China (12571187).

for time-periodic equations. In particular, Ref. [14] shows an explicit formula of the second-order Melnikov function which can be computable in applications.

More complicated than homoclinic tangles, heteroclinic tangles create from transversal intersections of stable and unstable manifolds associated with different saddles. For example, if a diffeomorphism possesses n heteroclinic points and forms a transversal n-cycle, then it implies a transversal homoclinic point and chaos arising [18]. This paper studies dynamics of van der Pol equation on torus which admits four heteroclinic solutions to two saddles. We consider periodically forced van der Pol equation. We present, through numerical simulations, chaotic heteroclinic tangles with the first-order Melnikov function and the second-order Melnikov function.

2. High order Melnikov's method

We consider as identical all points whose coordinates differ by 2π, and use $\mathbb{T} = [-\pi, \pi] \times [-\pi, \pi]$ to denote the torus. The forced van der Pol equation on torus $\mathbb{T}$ can be written in the form

$$\begin{aligned} \dot{x} &= \sin y, \\ \dot{y} &= -\sin x + \varepsilon P(x, y, t), \end{aligned} \tag{2.1}$$

where $P(x, y, t)$ is a real analytic bounded function in $(x, y) \in \mathbb{T}$ and T-periodic in t. Suppose ε is a small parameter, so that eq.(2.1) is a perturbation of autonomous equation

$$\begin{aligned} \dot{x} &= \sin y, \\ \dot{y} &= -\sin x, \end{aligned} \tag{2.2}$$

which has four singular points at $O(0, 0)$, $O_1(\pm\pi, 0)$, $O_2(0, \pm\pi)$ and $O_3(\pm\pi, \pm\pi)$. Within the four singular points, O and O_3 are centers while O_1 and O_2 are saddle points. Moreover, there are four heteroclinic orbits connecting O_1 and O_2, forming a heteroclinic cycle. Fig.1 depicts the phase structure on the plane and on the cylinder. The heteroclinic cycle divides the torus into two regions, one surrounding O and the other surrounding O_3. Let ℓ_{12} denote the heteroclinic orbit from $O_1(-\pi, 0)$ to $O_2(0, \pi)$, and ℓ_{21} the heteroclinic orbit from $O_2(0, \pi)$ to $O_1(\pi, 0)$. By symmetry, we denote the other two heteroclinic orbits by $-\ell_{12}$ and $-\ell_{21}$.

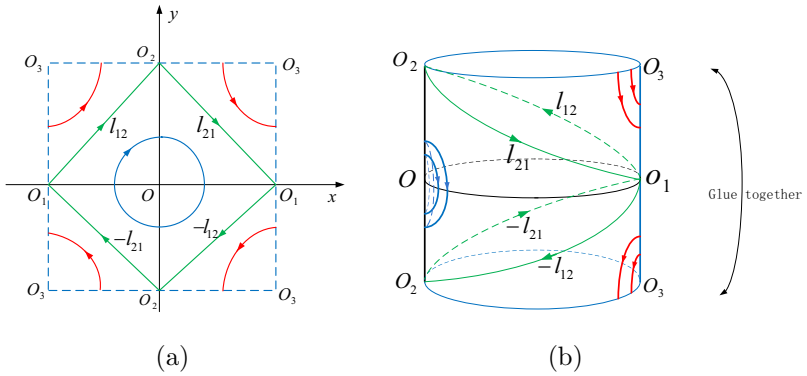

Figure 1. The phase portrait of eq.(2.2): (a)on the plane. (b)on the cylinder.

In fact, eq.(2.2) is a Hamiltonian system with Hamiltonian energy

$$H(x,y) = \cos x + \cos y.$$

Then we solve the heteroclinic orbit ℓ_{12} and write it down as

$$\ell_{12} := \ell_{12}(t) = \{(a(t), b(t)) : t \in R\},$$

where

$$a(t) = 2\arctan e^t - \pi, \quad b(t) = 2\arctan e^t. \tag{2.3}$$

A direct computation shows that $\ell_{21} := \ell_{21}(t) = \{(b(t), -a(t)) : t \in R\}$.

For eq.(2.1), we consider the splitting heteroclinic orbit ℓ_{12} to introduce the high order Melnikov method. We denote by $W^u_\varepsilon(O_1)$ the unstable manifold of O_1 and $W^s_\varepsilon(O_2)$ the stable manifold of O_2. For simplicity we call Melnikov function "M function". For a given section time $t_0 \in [0, T)$, the splitting distance between $W^u_\varepsilon(O_1)$ and $W^s_\varepsilon(O_2)$ is assumed to be [14]

$$D(t_0, \varepsilon) = E_0(t_0) + \varepsilon E_1(t_0) + \cdots + \varepsilon^n E_n(t_0) + \cdots, \tag{2.4}$$

where $E_0(t_0)$ is the first-order M function, and $E_1(t_0)$ the second-order M function. In general, we use $E_n(t_0)$ to denote the $(n+1)$th-order M function$(n \geq 0)$.

Remark 2.1. $E_0(t_0) = C \cdot M_0(t_0)$ where $C \neq 0$ is a constant.

We have the following theorem:

Theorem 2.1. *For eq.(2.1), suppose that $P(x, y, t)$ satisfies*

$$P(O_i, t) = 0, \quad i = 1, 2, \quad \forall t \in R. \tag{2.5}$$

Then, for the splitting heteroclinic orbit ℓ_{12}, the second-order M function $E_1(t_0)$ is given by

$$\begin{aligned} E_1(t_0) = &- \frac{P(\ell_{12}(0), t_0)}{2\dot{a}(0)} E_0(t_0) - \int_{-\infty}^{+\infty} \int_0^t \dot{a}(t) P(\ell_{12}(t), t+t_0) P_y(\ell_{12}(\tau), \tau+t_0)\, d\tau dt \\ &- \frac{1}{2} \int_{-\infty}^{+\infty} \int_0^t \frac{\dot{a}(t)}{\dot{a}(\tau)} \big[P(\ell_{12}(t), t+t_0) P_t(\ell_{12}(\tau), \tau+t_0) \\ &+ P(\ell_{12}(\tau), \tau+t_0) P_t(\ell_{12}(t), t+t_0) \big]\, d\tau dt, \end{aligned} \tag{2.6}$$

where $E_0(t_0)$ is the first-order M function in (2.4), and

$$\begin{aligned} P_y(\ell_{12}(\tau), \tau + t_0) &= \frac{\partial P(x, y, t)}{\partial y}|_{(x,y,t)=(\ell_{12}(\tau),\tau+t_0)}, \\ P_t(\ell_{12}(\tau), \tau + t_0) &= \frac{\partial P(x, y, t)}{\partial t}|_{(x,y,t)=(\ell_{12}(\tau),\tau+t_0)}. \end{aligned} \tag{2.7}$$

Proof. Let $D_{\ell_{12}}$ be a neighborhood of the splitting heteroclinic orbit ℓ_{12}, and L be a straight line normal to ℓ_{12} and through $O(0, 0)$. Referring to Fig.2 we see that

$$L = \{(x, y)|x + y = 0\}.$$

Then each solution starting in $D_{\ell_{12}}$ evolves forward to O_2 and backward to O_1. By the existence and uniqueness theorem of solution, for a given section time $t_0 \in [0, T)$, there exists a unique stable solution $(x^s(t, \varepsilon), y^s(t, \varepsilon))$ starting on L. Also, there exists a unique unstable solution $(x^u(t, \varepsilon), y^u(t, \varepsilon))$ starting on L. Then we denote $p^+ = (x^s(t_0, \varepsilon), y^s(t_0, \varepsilon))$ and $p^- = (x^u(t_0, \varepsilon), y^u(t_0, \varepsilon))$. Clearly, $p^+, p^- \in L$. From [14], the splitting distance $D(t_0, \varepsilon)$ between $W^s_\varepsilon(O_2)$ and $W^u_\varepsilon(O_1)$ is defined as

$$D(t_0, \varepsilon) = \frac{H(p^+) - H(p^-)}{\varepsilon}, \tag{2.8}$$

where $H(x, y) = \cos x + \cos y$ is the Hamiltonian of eq.(2.2).

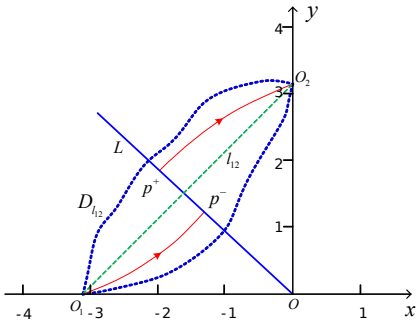

Figure 2. The neighborhood of ℓ_{12} and the straight line L.

After a time shift t_0, we let $x(t) = x^s(t + t_0, \varepsilon)$ and $y(t) = y^s(t + t_0, \varepsilon)$. Then, $(x(t), y(t))$ is a solution of the following shifted equation

$$\begin{aligned} \dot{x} &= \sin y, \\ \dot{y} &= -\sin x + \varepsilon P(x, y, t + t_0), \end{aligned} \tag{2.9}$$

such that $(x(0), y(0)) \in L$. To solve $(x(t), y(t))$ in eq.(2.9) we turn to solve the perturbed energy $H(x(t), y(t))$.

Remark 2.2.

(i) Originally, $H(x, y)$ is the Hamiltonian of unperturbed equation (2.2). Now for the perturbed solution $(x(t), y(t))$, the energy $H(x(t), y(t))$ is the original Hamiltonian evaluated along the perturbed orbits.

(ii) The time variation of $H(x(t), y(t))$ reflects the leading-order effect of the perturbation.

Setting $\mathbb{H}(t, t_0, \varepsilon) = \varepsilon^{-1} H(x(t), y(t))$, and differentiating $\mathbb{H}(t, t_0, \varepsilon)$ with respect to t yields

$$\frac{\partial \mathbb{H}(t, t_0, \varepsilon)}{\partial t} = -\sin y(t) \cdot P(x(t), y(t), t + t_0). \tag{2.10}$$

Using $\varepsilon \mathbb{X}(t) = x(t) - a(t)$, $\varepsilon \mathbb{Y}(t) = y(t) - b(t)$ and $\lim_{t \to +\infty} \mathbb{H}(t, t_0, \varepsilon) = 0$, we integrate eq.(2.10) to obtain

$$\mathbb{H}(t, t_0, \varepsilon) = \int_t^{+\infty} \sin(b(\tau) + \varepsilon \mathbb{Y}(\tau)) \cdot P(a(\tau) + \varepsilon \mathbb{X}(\tau), b(\tau) + \varepsilon \mathbb{Y}(\tau), \tau + t_0) d\tau. \tag{2.11}$$

Indeed, $\mathbb{H}(t, t_0, \varepsilon)$ is an energy solution featuring the stable manifold $W^s_\varepsilon(O_2)$. Expanding $\mathbb{H}(t, t_0, \varepsilon)$ in the power series of ε, the coefficient in front of ε^1 reads

$$\int_t^{+\infty} \{\sin b(\tau) \mathcal{P}_x(\tau, t_0) \mathbb{X}_0 + [\cos b(\tau) \mathcal{P}(\tau, t_0) + \sin b(\tau) \mathcal{P}_y(\tau, t_0)] \mathbb{Y}_0\} d\tau, \tag{2.12}$$

where $\mathcal{P}(\tau, t_0) = P(a(\tau), b(\tau), \tau + t_0)$, $\mathcal{P}_x(\tau, t_0) = P_x(a(\tau), b(\tau), \tau + t_0)$, $\mathcal{P}_y(\tau, t_0) = P_y(a(\tau), b(\tau), \tau + t_0)$, and

$$\begin{aligned} \mathbb{X}_0 + \mathbb{Y}_0 &= \dot{a}(\tau) \int_0^\tau \frac{\mathcal{P}(t, t_0)}{\dot{a}(t)} dt, \\ \mathbb{X}_0 - \mathbb{Y}_0 &= \frac{1}{\dot{a}(\tau)} \int_\tau^{+\infty} \dot{a}(t) \mathcal{P}(t, t_0) dt. \end{aligned} \tag{2.13}$$

Denote

$$E_1(t, t_0) = \int_t^{+\infty} \{\sin b(\tau) \mathcal{P}_x(\tau, t_0) \mathbb{X}_0 + [\cos b(\tau) \mathcal{P}(\tau, t_0) + \sin b(\tau) \mathcal{P}_y(\tau, t_0)] \mathbb{Y}_0\} d\tau. \tag{2.14}$$

To present the formula in theorem 2.1 we need a lemma. First we denote

$$\begin{aligned} f_1(\tau) &= \frac{1}{\dot{a}(\tau)} [\sin b(\tau) \mathcal{P}_x(\tau, t_0) - \sin b(\tau) \mathcal{P}_y(\tau, t_0) - \cos b(\tau) \mathcal{P}(\tau, t_0)], \\ f_2(\tau) &= \dot{a}(\tau) [\sin b(\tau) \mathcal{P}_x(\tau, t_0) + \sin b(\tau) \mathcal{P}_y(\tau, t_0) + \cos b(\tau) \mathcal{P}(\tau, t_0)]. \end{aligned}$$

Lemma 2.1.

$$\begin{aligned} f_1(\tau) &= \left(\frac{\mathcal{P}(\tau, t_0)}{\dot{a}(\tau)} \right)' - 2\mathcal{P}_y(\tau, t_0) - \frac{\mathcal{P}_t(\tau, t_0)}{\dot{a}(\tau)}, \\ f_2(\tau) &= (\dot{a}(\tau) \mathcal{P}(\tau, t_0))' - \dot{a}(\tau) \mathcal{P}_t(\tau, t_0). \end{aligned}$$

Remark 2.3. The prime in Lemma 2.1 means the derivative with respect to τ.

From (2.14) we find that

$$\begin{aligned}&E_1(t,t_0)\\=&\frac{1}{2}\int_t^{+\infty} f_1(\tau)\cdot\int_\tau^{+\infty}\sin b(s)\mathcal{P}(s,t_0)dsd\tau+\frac{1}{2}\int_t^{+\infty} f_2(\tau)\cdot\int_0^{\tau}\frac{\mathcal{P}(s,t_0)}{\sin b(s)}dsd\tau.\end{aligned}\tag{2.15}$$

Using Lemma 2.1 we have

$$\begin{aligned}E_1(t,t_0)=&-\frac{1}{2}\frac{\mathcal{P}(t,t_0)}{\dot a(t)}\int_t^{+\infty}\sin b(s)\mathcal{P}(s,t_0)ds\\&-\int_t^{+\infty}\int_\tau^{+\infty}\mathcal{P}_y(\tau,t_0)\sin b(s)\mathcal{P}(s,t_0)dsd\tau\\&-\frac{1}{2}\int_t^{+\infty}\int_0^{\tau}\frac{\dot a(\tau)}{\dot a(s)}[\mathcal{P}(\tau,t_0)\mathcal{P}_t(s,t_0)+\mathcal{P}(s,t_0)\mathcal{P}_t(\tau,t_0)]dsd\tau\\&-\frac{\dot a(t)\mathcal{P}(t,t_0)}{2}\int_0^t\frac{\mathcal{P}(s,t_0)}{\sin b(s)}ds.\end{aligned}\tag{2.16}$$

Putting $t=0$ in (2.16) yields

$$\begin{aligned}&E_1(0,t_0)\\=&-\frac{\mathcal{P}(0,t_0)}{2\dot a(0)}\int_0^{+\infty}\sin b(s)\mathcal{P}(s,t_0)ds-\int_0^{+\infty}\int_0^{s}\mathcal{P}_y(\tau,t_0)\sin b(s)\mathcal{P}(s,t_0)d\tau ds\\&-\frac{1}{2}\int_0^{+\infty}\int_0^{\tau}\frac{\dot a(\tau)}{\dot a(s)}[\mathcal{P}(\tau,t_0)\mathcal{P}_t(s,t_0)+\mathcal{P}(s,t_0)\mathcal{P}_t(\tau,t_0)]dsd\tau.\end{aligned}\tag{2.17}$$

We see that $E_1(0,t_0)$ is the initial value of the second-order M function on the stable manifold $W^s_\varepsilon(O_2)$. For simplicity, we write $E_1^+(t_0)\triangleq E_1(0,t_0)$. In the same way, on the unstable manifold $W^u_\varepsilon(O_1)$, we have the corresponding $E_1^-(t_0)$. Then $E_1(t_0)=E_1^+(t_0)-E_1^-(t_0)$ is exactly the formula in Theorem 2.1. □

Remark 2.4.

(i) The formula $E_1(t_0)$ in Theorem 2.1 is for the van der Pol equation (2.1), which differs from the polynomial equations in the Refs. [14, 19].

(ii) By defining the separation between $W^s_\varepsilon(O_2)$ and $W^u_\varepsilon(O_1)$ on the line segment L, the proof somewhat simplifies those in the Refs. [14, 19].

3. Two concrete examples

Now we consider the perturbation $P(x,y,t)=(\sin x+\sin y)\cos\omega t$, and rewrite eq.(2.1) as

$$\begin{aligned}\dot x&=\sin y,\\\dot y&=-\sin x+\varepsilon(\sin x+\sin y)\cos\omega t.\end{aligned}\tag{3.1}$$

For eq.(3.1), we have the following proposition:

Proposition 3.1. *For small parameter ε, there exists a transverse homoclinic solution on the torus $\mathbb{T}$ such that chaotic dynamics occurs in the sense of Smale horseshoes.*

Proof. We first analyze it on the plane, and then project it onto the torus. For the splitting heteroclinic orbit ℓ_{21}, let $W^u_\varepsilon(O_2)$ be the unstable manifold of O_2 and $W^s_\varepsilon(O_1)$ be the stable manifold of O_1. For the symmetric heteroclinic orbits $-\ell_{12}$ and $-\ell_{21}$, we use $\overline{W}^u_\varepsilon(O_1)$, $\overline{W}^s_\varepsilon(O_2)$ and $\overline{W}^u_\varepsilon(O_2)$, $\overline{W}^s_\varepsilon(O_1)$ to denote the corresponding unstable and stable manifolds; see Fig.3.

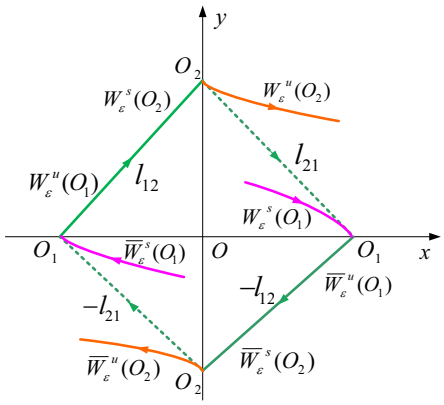

Figure 3. The stable and unstable manifolds of $O_1(\pm\pi, 0)$ and $O_2(0, \pm\pi)$.

Recall that the first-order M function $E_0(t_0)$ reads [1]

$$E_0(t_0) = \int_{-\infty}^{+\infty} \sin b(t) \cdot P(a(t), b(t), t + t_0)dt. \tag{3.2}$$

Applying $E_0(t_0)$ both to the heteroclinic orbits ℓ_{21} and $-\ell_{21}$ gives

$$E_0(t_0) = \frac{4\pi\omega e^{-\frac{\omega\pi}{2}}}{1 - e^{-\omega\pi}} \cos\omega t_0. \tag{3.3}$$

From (3.3), $E_0(t_0)$ has a simple zero at $t_0^* = \frac{\pi}{2\omega}$. Then, for ε sufficiently small, $W^u_\varepsilon(O_2)$ intersects $W^s_\varepsilon(O_1)$ transversely, and $\overline{W}^u_\varepsilon(O_2)$ intersects $\overline{W}^s_\varepsilon(O_1)$ transversely.

On the other hand, we have

$$\dot{a}(t) = \sin b(t), \quad \dot{b}(t) = -\sin a(t), \ \forall t \in R, \tag{3.4}$$

since ℓ_{12} is a heteroclinic solution of eq.(2.2). From (2.3) we find that $b(t) = a(t) + \pi$ for every $t \in R$, which implies that $\sin a(t) + \sin b(t) \equiv 0$ for every $t \in R$. Combining (3.1) with (3.4), the heteroclinic orbit ℓ_{12} remains a solution of eq.(3.1). In the same way, the symmetric heteroclinic orbit $-\ell_{12}$ remains a solution of eq.(3.1). Therefore, due to the work of [18], there exists a transverse homoclinic solution for eq.(3.1). Under the natural projection of R^2 onto $\mathbb{T}$, there exists a transverse homoclinic solution on the torus $\mathbb{T}$. From Smale-Birkhoff theorem [1], chaotic dynamics arises in the sense of horseshoes on $\mathbb{T}$. □

Fig.4 plots, at parameter $\varepsilon = 0.5$, $\omega = 6$ and initial value $(x_0, y_0) = (-3.14, 0.0)$, the Poincaré map on the plane and on the torus for eq.(3.1). From Fig.4 we know that the infinite number of points on the Poincaré map correspond to the complicated or chaotic dynamics of eq.(3.1), claiming the existence of homoclinic tangles in Prop.3.1. Fig.5 is the Lyapunov exponents spectrum. Our simulations are performed using the fourth-order Runge-Kutta routine for fixed parameters $(\varepsilon, \omega) = (0.5, 6)$. We pick the initial value at $(x_0, y_0) = (-3.14, 0.0)$ and $t_0 = 0$. We set the time step $\Delta t = 0.01$. The largest Lyapunov exponent, at $t = 1000$, is approximately $L_1 \approx 0.0144$. $L_1 > 0$ implies that eq.(3.1) occurs chaotic dynamics.

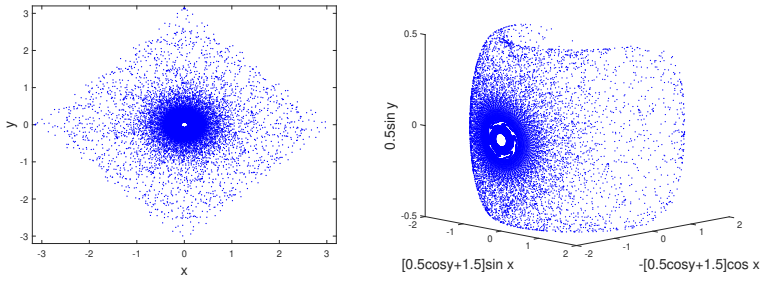

(a) (b)

Figure 4. The Poincaré map for eq.(3.1) at $\varepsilon = 0.5$, $\omega = 6$, $(x_0, y_0) = (-3.14, 0.0)$:(a) on the plane; (b)on the torus $\mathbb{T}$.

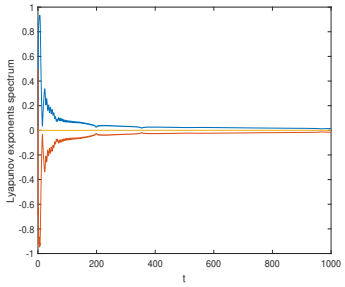

Figure 5. The Lyapunov exponents spectrum for eq.(3.1) at $\varepsilon = 0.5$, $\omega = 6$, $(x_0, y_0) = (-3.14, 0.0)$.

Furthermore, we consider the perturbation $P(x, y, t) = (\sin x + \gamma \sin^3 x) \cos \omega t$ with $\gamma \in R$. Then eq.(2.1) becomes

$$\begin{aligned} \dot{x} &= \sin y, \\ \dot{y} &= -\sin x + \varepsilon(\sin x + \gamma \sin^3 x) \cos \omega t. \end{aligned} \tag{3.5}$$

Denote $\gamma_0 = -\frac{6}{\omega^2+4}$. We have the following proposition:

Proposition 3.2. *At parameter $\gamma = \gamma_0$, eq.(3.5) admits, for small parameter ε, a transverse homoclinic solution such that chaotic dynamics occurs on the torus $\mathbb{T}$ in the sense of Smale horseshoes.*

Proof. We first apply the first-order M function $E_0(t_0)$ in (3.2) to both ℓ_{12} and $-\ell_{12}$, and obtain

$$E_0(t_0) = -\frac{\pi\omega e^{-\frac{\omega\pi}{2}}}{1-e^{-\omega\pi}}[2+\gamma\frac{4+\omega^2}{3}]\cos\omega t_0. \tag{3.6}$$

Similarly, applying $E_0(t_0)$ to both ℓ_{21} and $-\ell_{21}$ gives

$$E_0(t_0) = \frac{\pi\omega e^{-\frac{\omega\pi}{2}}}{1-e^{-\omega\pi}}[2+\gamma\frac{4+\omega^2}{3}]\cos\omega t_0. \tag{3.7}$$

From (3.6) and (3.7) we denote

$$\gamma_0 = -\frac{6}{(4+\omega^2)},$$

which implies that, at $\gamma = \gamma_0$, $E_0(t_0)$ in both (3.6) and (3.7) vanishes for every $t_0 \in [0, \frac{2\pi}{\omega})$. Thus, for eq.(3.5), we can not detect heteroclinic tangles by the first-order M function $E_0(t_0)$.

Next we turn to evaluate the second-order M function $E_1(t_0)$ related to the four heteroclinic orbits. Since $P(x,y,t) = \sin x(1+\gamma_0\sin^2 x)\cos\omega t$ at $\gamma = \gamma_0$, we have $E_0(t_0) \equiv 0$ and $P_y(x(\tau), y(\tau), \tau + t_0) \equiv 0$ for every $t_0 \in [0, \frac{2\pi}{\omega})$. Then $E_1(t_0)$ in Theorem 2.1 simplifies to

$$\begin{aligned} E_1(t_0) = &-\frac{1}{2}\int_{-\infty}^{+\infty}\int_0^t \frac{\dot a(t)}{\dot a(\tau)}[P(\ell_{12}(t), t+t_0)P_t(\ell_{12}(\tau), \tau+t_0) + P(\ell_{12}(\tau), \tau+t_0) \\ &P_t(\ell_{12}(t), t+t_0)]d\tau dt. \end{aligned} \tag{3.8}$$

Putting $P_t(x,y,t) = -\omega\sin x(1+\gamma_0\sin^2 x)\sin\omega t$ to (3.8) yields

$$E_1(t_0) = \frac{\omega}{2}I_1(\omega,\gamma_0)\cos 2\omega t_0, \tag{3.9}$$

where

$$I_1(\omega,\gamma_0) = \int_{-\infty}^{+\infty}\int_0^t \sin^2 b(t)[1+\gamma_0\sin^2 b(t)][1+\gamma_0\sin^2 b(\tau)]\cdot\sin\omega(t+\tau)d\tau dt. \tag{3.10}$$

By straightforward computations we find that

$$I_1(\omega,\gamma_0) = \frac{\omega}{2} + \mathcal{O}(\omega^3). \tag{3.11}$$

Therefore,

$$E_1(t_0) = [\frac{\omega^2}{4} + \mathcal{O}(\omega^4)]\cos 2\omega t_0, \tag{3.12}$$

which has a simple zero at $t_0^* = \frac{\pi}{4\omega}$. That is to say, $E_1(t_0^*) = 0$ but $\frac{dE_1(t_0^*)}{dt_0} \neq 0$. By implicit function theorem, there exists a unique function $t_0 = t_0(\varepsilon)$ such that

$$D(t_0(\varepsilon),\varepsilon) = \varepsilon E_1(t_0(\varepsilon)) + \cdots + \varepsilon^n E_n(t_0(\varepsilon)) + \cdots \equiv 0, \quad \forall\varepsilon \in (-\varepsilon_0, \varepsilon_0). \tag{3.13}$$

This means that, for sufficiently small ε, the unstable manifold $W^u_\varepsilon(O_1)$ intersects the stable manifold $W^s_\varepsilon(O_2)$ transversely.

By symmetry, at $\gamma = \gamma_0$, the second-order M function $E_1(t_0)$ for the splitting heteroclinic orbit $-\ell_{12}$ is the same as (3.12), i.e.

$$E_1(t_0) = [\frac{\omega^2}{4} + \mathcal{O}(\omega^4)] \cos 2\omega t_0. \tag{3.14}$$

In the same way, for the splitting heteroclinic orbit ℓ_{21} and its symmetric $-\ell_{21}$, the second-order M function $E_1(t_0)$ appears

$$E_1(t_0) = -[\frac{\omega^2}{4} + \mathcal{O}(\omega^4)] \cos 2\omega t_0. \tag{3.15}$$

Combining the equalities (3.12), (3.14) with (3.15) we conclude that, at parameter $\gamma = \gamma_0$, the stable and unstable manifolds for the splitting heteroclinic orbits ℓ_{12}, ℓ_{21}, $-\ell_{12}$ and $-\ell_{21}$ intersect each other transversely. From Ref. [18] and the Smale-Birkhoff theorem [1], eq.(3.5) admits a transverse homoclinic solution such that chaotic dynamics occurs on the torus in the sense of Smale horseshoes. □

Fig.6 shows that for eq.(3.5), at $\varepsilon = 0.5$, $\omega = 10$ and initial conditions $(x_0, y_0) = (-3.14, 0.0)$, the Poincaré map on the plane and on the torus. Also, the infinite number of points on the Poincaré map in Fig.6 demonstrates the chaotic dynamics of eq.(3.5), which was claimed in Prop.3.2. Fig.7 presents the time series of $x(t)$, the Fourier spectrum and the Lyapunov exponents spectrum. Using the fourth-order Runge-Kutta routine, we perform our simulations for fixed parameters $(\varepsilon, \omega) = (0.5, 10)$. The time step and initial values are the same as in Fig.5. The largest Lyapunov exponent for eq.(3.5), at $t = 1000$, is approximately $L_1 \approx 0.0079$. $L_1 > 0$ implies that eq.(3.5) exhibits chaotic dynamics.

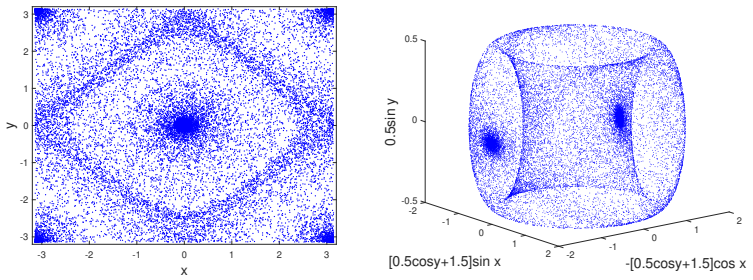

(a) (b)

Figure 6. The Poincaré map for eq.(3.5), at $\varepsilon = 0.5$, $\omega = 10$,$(x_0, y_0) = (-3.14, 0.0)$: (a)on the plane; (b)on the torus $\mathbb{T}$.

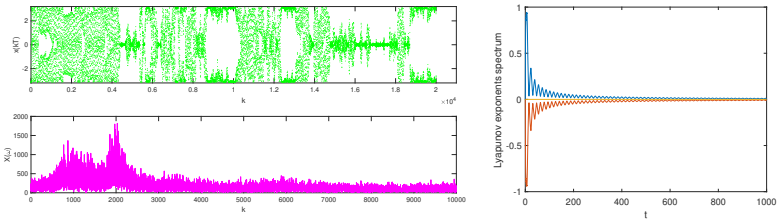

(a) (b)

Figure 7. For eq.(3.5), at $\varepsilon = 0.5$, $\omega = 10$, $(x_0, y_0) = (-3.14, 0.0)$. (a)The time evolution of $x(t)$ and its Fourier spectrum. (b)The Lyapunov exponents spectrum.

4. Conclusions

In our study, we have investigated chaotic tangles on the torus for periodic forced van der Pol equation. We have derived theoretically an explicit and computable formula of the second-order Melnikov function, which is useful when the classical Melnikov function fails to detect chaotic dynamics. Additionally, we have observed numerical simulations revealing chaotic heteroclinic tangles for two examples. We conclude that, from the energy point of view, high order Melnikov theory might open the way to more applications in certain fields.

Acknowledgements

The authors are much obliged to the anonymous reviewers for their careful reading, useful comments and constructive suggestions for the improvement of the manuscript of the present research work.

References

[1] J. Guckenheimer and P. Holmes, *Nonlinear oscillations, dynamical systems, and bifurcations of vector fields*, Springer Science & Business Media, New York, 2013.

[2] N. Levinson, *A second-order differential equation with singular solutions*, Annals of Mathematics, 1949, 50, 127–153.

[3] M. Levi, *Qualitative analysis of the periodically forced relaxation oscillations*, American Mathematical Society., 1981, 214, 1–147.

[4] S. Smale, *Differentiable dynamical systems*, Bulletin of the American mathematical Society, 1967, 73(6), 747–817.

[5] Q. Wang and L.-S. Young, *Toward a theory of rank one attractors*, Annals of Mathematics, 2008, 167, 349–480.

[6] Q. Wang and A. Oksasoglu, *Dynamics of homoclinic tangles in periodically perturbed second-order equations*, Journal of Differential Equations, 2011, 250(2), 710–751.

[7] F. Chen, A. Oksasoglu and Q. Wang, *Heteroclinic tangles in time-periodic equations*, Journal of differential Equations, 2013, 254(3), 1137–1171.

[8] O. Gjata and F. Zanolin, *An Application of the Melnikov Method to a Piecewise Oscillator*, Contemporary Mathematics, 2023, 4(2), 249–269.

[9] H. Li, Y. Shen, J. Li, et al. *On the Melnikov method for fractional-order systems*, Chaos, Solitons and Fractals, 2024, 188(115602).

[10] C.E. Papoutsellis, Y.-M. Scolan and R. Hascoët, *Capsize criteria in beam seas: Melnikov analysis vs. safe basin erosion*, Ocean Engineering, 2024, 306(118024).

[11] J.R.C. Piqueira, *Melnikov's method applied to accidental phase modulation phenomenon*, The European Physical Journal Special Topics, 2021, 230(18), 3449–3456.

[12] V.K. Melnikov, *On the stability of the center for time periodic perturbations*, Transactions of the Moscow Mathematical Society, 1963, 12, 1–56.

[13] S. Lenci and R. Giuseppe, *Higher-order Melnikov functions for single-DOF mechanical oscillators: theoretical treatment and applications*, Mathematical Problems in Engineering, 2004(2), 145–168.

[14] F. Chen and Q. Wang, *High order Melnikov method: Theory and application*, Journal of Differential Equations, 2019, 267(2), 1095–1128.

[15] F. Chen and Q. Wang, *High-order Melnikov method for time-periodic equations*, Advanced Nonlinear Studies, 2017, 17(4), 793–818.

[16] Q. Wang, *Exponentially small splitting: a direct approach*, Journal of Differential Equations, 2020, 269(1): 954–1036.

[17] A. Oksasoglu and Q. Wang, *High order Melnikov method: pendulums*. Journal of Differential Equations, 2022, 312, 176–208.

[18] Y. Yan and M. Qian, *Transversal heteroclinic cycle and its application to Hénon mapping*, Chinese Science Bulletin, 1985, 13, 961–965.

[19] Y. Zhong and F. Chen, *Chaotic heteroclinic tangles with the degenerate Melnikov function*, Nonlinear Dynamics, 2022, 108(1), 697–709.